

K. Mitra

S. Kumar

A. Vedavarz

M. K. Moallemi

Department of Mechanical Engineering,
Polytechnic University,
6 Metrotech Center,
Brooklyn, NY 11201

Experimental Evidence of Hyperbolic Heat Conduction in Processed Meat

The objective of this paper is to present experimental evidence of the wave nature of heat propagation in processed meat and to demonstrate that the hyperbolic heat conduction model is an accurate representation, on a macroscopic level, of the heat conduction process in such biological material. The value of the characteristic thermal time of a specific material, processed bologna meat, is determined experimentally. As a part of the work different thermophysical properties are also measured. The measured temperature distributions in the samples are compared with the Fourier results and significant deviation between the two is observed, especially during the initial stages of the transient conduction process. The measured values are found to match the theoretical non-Fourier hyperbolic predictions very well. The superposition of waves occurring inside the meat sample due to the hyperbolic nature of heat conduction is also proved experimentally.

Introduction

The traditional Fourier heat conduction equation implies an infinite speed of propagation of the thermal wave, indicating that a local change in temperature causes an instantaneous perturbation in the temperature at each point in the medium, even if the intervening distances are large. To consider the finite speed of wave propagation, a damped wave model is proposed in the literature by using a variety of reasonings and derivations. Its development is presented in detail in the review articles by Joseph and Preziosi (1989, 1990). According to this formulation, the heat flux equilibrates to the imposed temperature gradient via a relaxation phenomenon characterized by a thermal relaxation or thermal characteristic time. From the point of view of heat transfer in materials with nonhomogeneous inner structures such as biological materials, the thermal characteristic time can be defined as the time necessary for accumulating thermal energy required for propagative heat transfer to a particular point in the medium (Kaminski, 1990). The value of this characteristic time is of importance since conduction processes that occur for time periods of the order of the thermal characteristic time may exhibit significant non-Fourier behavior.

Many studies in the literature have considered mathematical solutions to a variety of problems via hyperbolic conduction models (Joseph and Preziosi, 1989, 1990; Wiggert, 1977; Kim et al., 1990; Rastegar, 1989; Kar et al., 1992). Thermodynamic validity of the hyperbolic equations and the range of parameters where non-Fourier considerations are important have also been recently considered (Lavine and Bai, 1994; Vedavarz et al., 1994a, b). The thermal characteristic time for meat products was estimated to be on the order of 20–30 seconds (Kaminski, 1990) but its value has not been measured. In addition, no work is reported that directly validates the hyperbolic nature of heat conduction in biological materials by comparing experimentally observed temperature or flux distributions with the non-Fourier predictions. Recently Tzou (1992) compared the wave solution for the temperature rise induced by a propagating crack tip in steel with the experimental results obtained by Zehnder and Rosakis (1991) to conclude the wave nature of heat conduction.

Four different experiments are reported here for different kinds of boundary conditions. The temperature histories of thermocou-

ples embedded in the samples are recorded and the experimental results show instantaneous jumps in temperatures when the heat waves reach the thermocouples. The phenomenon of superposition of waves occurring due to two heat waves approaching each other from two sides is verified. Both addition and subtraction of waves is observed. By comparing the experimental temperatures with theoretical predictions, the hyperbolic model is shown to be a valid macroscopic representation of the heat transfer in biological materials. The corresponding thermal characteristic time is found to be approximately 16 seconds. This large value of the characteristic time has significant implications in the modeling of many bio-heat transfer processes, especially in those that occur for short durations such as laser surgery.

Experiments Conducted

The value of the thermal characteristic time τ can be calculated theoretically for solids such as metals and dielectrics when the dominant heat carriers are either electrons or phonons (Ashcroft and Mermin, 1976; Vedavarz et al., 1994a). While there is no experimental method to measure the thermal characteristic time directly, the value for processed meat and other bio-materials can be found by measuring the thermal diffusivity and the penetration time. The penetration time, t_p , is the time required for the thermal wave to reach the specified location x_p within the medium. This implies that the velocity of the propagating wave can be determined as follows:

$$v = \frac{x_p}{t_p} \quad (1)$$

By knowing the wave velocity, the value of τ can be determined from the following relation (Kaminski, 1990):

$$\tau = \frac{\alpha}{v^2} \quad (2)$$

Here $\alpha = \kappa/\rho C$, where α is the thermal diffusivity, κ the thermal conductivity, ρ the density, and C the specific heat. To calculate the thermal characteristic time for the processed meat, κ , ρ , C , and v are to be measured.

The values of the different thermophysical parameters ascertained experimentally, including their uncertainties, are shown in Table 1. Thermal conductivity is determined by measuring the steady-state axial temperature gradients across cylindrical metallic bars of known thermal conductivities between which the sample is inserted. The temperature distribution is kept one dimen-

Contributed by the Heat Transfer Division for publication in the JOURNAL OF HEAT TRANSFER. Manuscript received by the Heat Transfer Division October 1992; revision received March 1994. Keywords: Conduction, Thermophysical Properties. Associate Technical Editor: R. Viskanta.

sional by insulating the outer cylindrical surfaces of the bar and the sample. The specific heat of the sample is measured by a Differential Scanning Calorimeter (Du Pont Instruments, Module 910 attached with 9900 computer model) over the temperature range of 5 to 30°C. The density is measured by measuring the mass of the sample by a sensitive mass balance and the volume of the sample.

The data acquisition (Model, HP 3497A) used is set on 0–0.1 V range with $5\frac{1}{2}$ digits resolution, implying least count of $1 \mu\text{V}$, which corresponds to 0.025°C when a T-type thermocouple is used. The data acquisition is calibrated against a function generator to study its response compared to the various applied pulses. Different pulses such as square wave and sinusoidal are applied and the output of the data acquisition is found to match well with the input signal of the function generator, which is also observed with an oscilloscope. All experiments use copper-constantan (T-type) thermocouples having wire diameter of 0.127 mm (0.05 in.) and a bead diameter of approximately three times the wire diameter. The thermocouples are individually calibrated against an alcohol-in-glass thermometer (having $\pm 0.05^\circ\text{C}$ uncertainty), which ensures an accuracy of $\pm 0.15^\circ\text{C}$.

The four different experimental configurations and their boundary conditions are schematically depicted in Fig. 1. The processed meat (bologna) samples are in the shape of finite cylinders of approximately 10 cm (4 in.) diameter. The samples are well insulated on all sides (except on the planar sides, which are in contact with each other) to prevent any radial heat flow. Adequate pressure is applied to ensure that perfect contact is established between the thermocouples and the samples and between the different contacting samples. High thermal conductivity grease is applied at the interfaces of contacting samples to eliminate the effect of thermal contact resistance. The thermocouple beads are also coated with thermal grease to enhance contact. The thermocouples are inserted radially so that the leads follow an isothermal path to minimize conduction losses. All the thermocouples are connected to a computerized data acquisition system. The samples that need to be cooled for establishing different initial temperature conditions are refrigerated along with the insulation and the embedded thermocouples to prevent any thermal inertia effects at the initial stages of the experiment. Each experiment is conducted a minimum of three times and the data are reported for one since the deviation between different runs is not phenomenologically significant and the experiments are repeatable. It is ensured that sufficient time elapsed between each experiment so that no temperature gradients are present in the sample.

As a validation of the experimental setup and data collection and processing, two identical aluminum samples (whose dimensions are the same as those of the meat samples) at different temperatures are brought in contact with each other. The measured temperature profiles match the Fourier predictions within the experimental uncertainty of the thermocouples ($\pm 0.2^\circ\text{C}$).

Experiment I. This experiment is conducted to show that heat waves take a finite time to reach a particular point inside the

Table 1 Experimentally measured properties of processed meat

Table 1. Experimentally measured properties of processed meat.		
Variable	Value	Units
Thermal conductivity κ	0.80 ± 0.04	W/m·K
Density ρ	1230 ± 10	kg/m ³
Specific heat C	4.66 ± 0.20	kJ/kg·K
Thermal diffusivity α	$1.40 \times 10^{-7} \pm 0.12 \times 10^{-7}$	m ² /s

meat sample contrary to the instantaneous heat propagation as predicted by the Fourier model. Two identical meat samples at different initial temperatures are brought into contact with each other. One sample is refrigerated to 8.2°C and the other is at room temperature of 23.1°C. Thermocouples are embedded in the cold sample and in the room temperature sample at distances of 6.6 and 6.3 mm, respectively, from the interface of contact. Thermocouples are also placed at the interface of the two samples.

Experiment II. This experiment is performed to demonstrate the wave superposition phenomenon (addition) occurring when two waves traveling toward each other meet within the sample. Three samples are brought into contact, two large refrigerated ones at 8.5°C and one thin room temperature sample of 17.4°C, so that the thin room temperature sample is sandwiched between the two large refrigerated ones. The room temperature sample, which is between the two cold samples, is much less in thickness than the cold samples to ensure that the heat wave has sufficient amplitude even after traversing the entire thickness of the thin sample. Thermocouples are placed at the interface of the cold and room temperature samples, as well as inside the samples. The thermocouple inside the room temperature sample is at a distance of 3.8 and 5.7 mm from the top and bottom cold samples, respectively.

Experiment III. This experiment is also performed to show wave superposition (subtraction) by using a setup similar to that in the previous experiment, but with initial temperatures selected to cause wave subtraction in the middle sample as opposed to wave addition in the previous experiment. The three samples arranged in the large-thin-large sequence are initially at 24.1°C, 14.3°C, and 6.2°C, respectively. The thermocouple inside the middle sample is at a distance of 3.2 and 7.2 mm from the top and bottom interfaces, respectively.

Experiment IV. This experiment also shows that heat waves have finite propagation speed (cf. Experiment I). A cold meat sample is brought into contact with a warm constant temperature aluminum plate as depicted in Fig. 1(b). The sample along with the insulation is first refrigerated to 8.1°C, which is lower than the temperature of the constant temperature plate maintained at 28.2°C. The temperature of the plate is controlled by circulating a coolant through a pipe network attached to the back of the plate. The coolant temperature is maintained by a constant temperature bath. Thermocouples are placed within the sample at distances of 6.6 and 14.0 mm from the contacting surface, and at the con-

Nomenclature

C	= specific heat	T	= temperature	x	= nondimensional space coordinates
d	= nondimensional thickness	v	= propagation wave velocity	∇	= gradient
D	= dimensional thickness	x	= space coordinate	Subscripts	
h_{cont}	= dimensional thermal contact conductance	x_p	= specified location	c	= cold temperature sample
q	= heat flux	α	= thermal diffusivity	f	= Fourier
Q	= nondimensional heat flux	ζ	= nondimensional time	i	= initial
R	= nondimensional contact resistance	θ	= nondimensional temperature	m	= medium temperature sample
t	= time	κ	= thermal conductivity	r	= room temperature sample
t_p	= penetration time	ρ	= density	ref	= reference temperature
		τ	= thermal characteristic time		

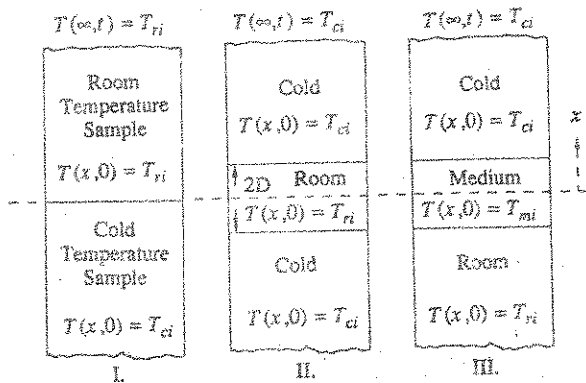


Fig. 1(a) Schematic of the experimental conditions for Experiments I, II, and III

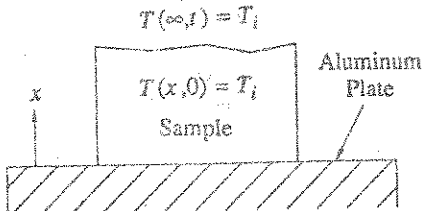


Fig. 1(b) Schematic of the experimental conditions for Experiment IV

act interface. The constant temperature plate also has many thermocouples embedded in it to monitor the plate temperature. The penetration time and propagation wave velocity is measured in the same manner as the experiments above.

Theoretical Profiles

Defining nondimensional variables as

$$\theta = \frac{T - T_i}{T_{ref} - T_i}, \quad Q = \frac{q\sqrt{\alpha\tau}}{\kappa(T_{ref} - T_i)}, \quad \chi = \frac{x}{\sqrt{\alpha\tau}}, \quad \zeta = \frac{t}{\tau}, \quad (3)$$

the hyperbolic conduction equation and the energy equation in a one-dimensional coordinate system are written as (Cattaneo, 1958; Joseph and Preziosi, 1989)

$$Q + \frac{\partial Q}{\partial \zeta} + \frac{\partial \theta}{\partial \chi} = 0, \quad \frac{\partial Q}{\partial \chi} + \frac{\partial \theta}{\partial \zeta} = 0. \quad (4)$$

Here θ is the nondimensional temperature; Q the nondimensional heat flux, ζ the nondimensional time, χ the nondimensional space coordinate, t the time, x the space coordinate, T the temperature, q the heat flux, T_{ref} the reference temperature, T_i the initial temperature, κ the thermal conductivity, C the specific heat, ρ the density, α the thermal diffusivity, and τ the thermal characteristic time of the processed meat.

The boundary and initial conditions used for obtaining the theoretical temperature profiles corresponding to the different experiments are shown in Figs. 1(a) and 1(b). In all the cases considered, the temperatures at large distances from the interface ($|x| \rightarrow \infty$) are taken equal to the corresponding initial temperatures. The temperature at the interface of contact between different samples is initially the mean of the adjacent samples, and for Experiment IV the interface temperature is taken as the temperature of the plate T_{plate} . The theoretical hyperbolic temperature profiles corresponding to the boundary and initial conditions of the different experiments conducted are obtained by the method of characteristics using Eq. (4). Details of the method are not presented here for brevity and can be found elsewhere (Wiggert, 1977). The theoretical nondimensional Fourier temperature pro-

files for the specified experiments are given as (Carslaw and Jaeger, 1959)

$$\theta_f = \operatorname{erfc} \left[\frac{\chi}{2\sqrt{\zeta}} \right],$$

$$T_{ref} = \frac{T_{ci} + T_ni}{2} \quad (I), \quad T_{ref} = T_{plate} \quad (IV), \quad (5)$$

$$\theta_f = \operatorname{erfc} \left[\frac{d + \chi}{2\sqrt{\zeta}} \right] + \operatorname{erfc} \left[\frac{d - \chi}{2\sqrt{\zeta}} \right],$$

$$T_{ref} = \frac{T_{ci} + T_ni}{2} \quad (II), \quad (6)$$

$$\theta_f = \operatorname{erfc} \left[\frac{d + \chi}{2\sqrt{\zeta}} \right] + \frac{T_{ci} - T_{n_i}}{T_{n_i} - T_{mi}} \operatorname{erfc} \left[\frac{d - \chi}{2\sqrt{\zeta}} \right],$$

$$T_{ref} = \frac{T_{ci} + T_{mi}}{2} \quad (III), \quad (7)$$

where $d = D/\sqrt{\alpha\tau}$ represents the nondimensional thickness of the sample sandwiched between the other two semi-infinite samples.

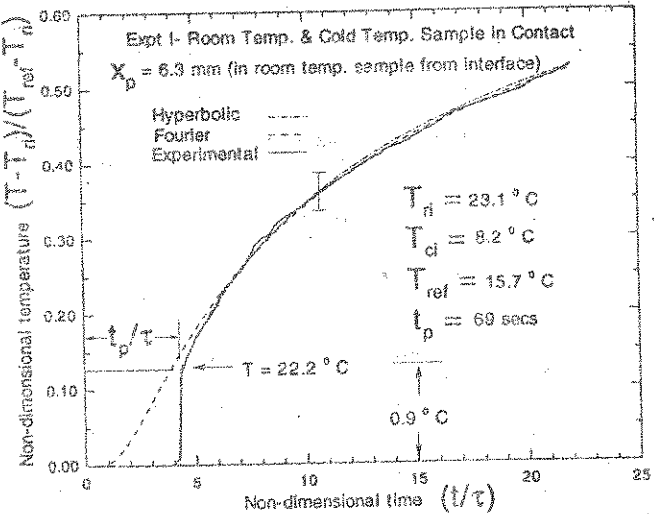


Fig. 2(a) Experimental results of nondimensional temperature versus time for Experiment I, for thermocouple at $x = 6.3$ mm

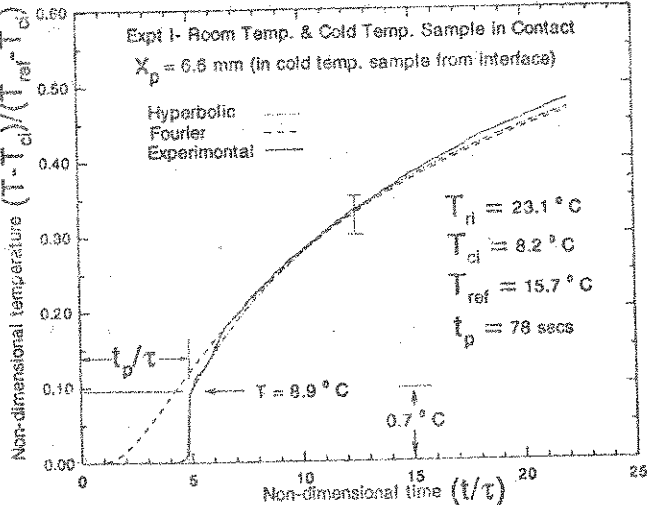


Fig. 2(b) Experimental results of nondimensional temperature versus time for Experiment I, for thermocouple at $x = 6.6$ mm

reading is $\pm 0.2^\circ\text{C}$, and the corresponding uncertainty in the thermocouple position and time readings are 0.3 mm and 0.5 second, respectively. The thermal time constant of the thermocouple is on the order of 0.05 second (Figliola and Beasley, 1991). Using Eqs. (1)–(2) and applying the uncertainty analysis, the value of τ obtained is in the range of 15–17 with an uncertainty of ± 2.1 seconds (13.6 percent). The results of the various experiments are tabulated in Table 2. However, it is worth mentioning that out of 38 experimental plots, 28 showed consistent penetration time t_p , 4 showed temperature jumps less than 0.2°C but consistent t_p , 2 showed large irregular jumps but consistent t_p , and 4 showed no jump in temperature.

The theoretical hyperbolic curves in Figs. 2–5 have been generated by the method of characteristics using the mean value of the experimentally determined values of τ , along with the other measured properties presented in Table 1 and 2. The theoretical Fourier curves are obtained via Eqs. (5)–(7).

The results for Experiment I are shown in Figs. 2(a) and 2(b). The experimental temperature profiles from thermocouples embedded in both the cold and room temperature samples exhibit strong non-Fourier behavior. In case of Experiment II, the results of the thermocouples inside the room temperature sample and at the interface of the cold and room temperature samples are reported in Figs. 3(a) and 3(b). The experimental data for the thermocouple in the middle sample, Fig. 3(a), clearly show two temperature jumps associated with the two wave fronts that originated from the two interfaces. The presence of the two jumps cannot be explained by classical Fourier theory and is only possible if the heat propagation is via heat waves and the jumps are a manifestation of the addition of the two positive amplitude waves via superposition. After the heat wave from one side reaches the point where the thermocouple is placed, it causes a jump in temperature, but the heat wave from the other end has not reached the point. The temperature then continues to increase until a second jump in temperature takes place when the heat wave from the other end of the sample reaches the point where the thermocouple is placed inside the room temperature sample. After that, the temperature continues to rise due to the combined effect of two waves. The result of the thermocouple placed at the interface of the cold and room temperature samples is shown in Fig. 3(b). The interface temperature attains the intermediate temperature $(T_{ci} + T_{ri})/2$ at the instant of contact and stays constant at this value until the wave generated by the other interface reaches it. At that instant the temperature exhibits a sharp jump and subsequently varies in accordance with hyperbolic wave pre-

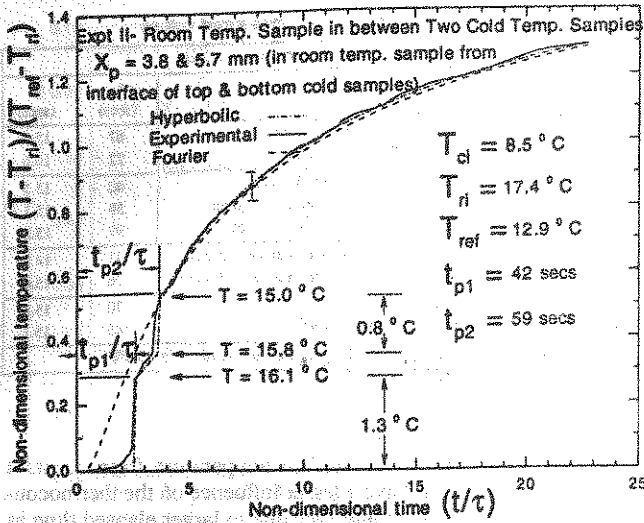


Fig. 3(a) Experimental results of nondimensional temperature versus time for Experiment II, for thermocouple at $x = 3.8$ and 5.7 mm from interface of top and bottom cold samples, respectively

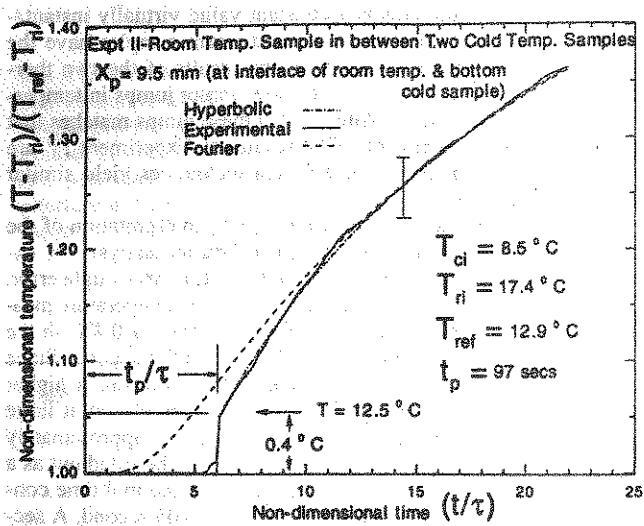


Fig. 3(b) Experimental results of nondimensional temperature versus time for Experiment II, for thermocouple at the interface of cold and room temperature samples

Results and Discussion

The results of the experiments described above offer compelling evidence of the wave nature of heat conduction in processed meat (bologna). The fact that a finite time occurs before the thermocouples embedded within the media register any temperature deviations, and that the temperature changes abruptly, indicate a wave behavior of the conduction mechanism in such material. These phenomena are clearly evident from the experimental data of Figs. 2–5. The superposition phenomenon of waves, which occurs due to two heat waves approaching from each other, is also experimentally verified as shown in Figs. 3(a) (addition of wave amplitudes) and 4 (subtraction of wave amplitudes).

The value of thermal characteristic time τ has been evaluated experimentally by noting the instant t_p at which the imposed temperature boundary condition causes the thermocouples located at x_p to display a significant deviation (i.e., greater than its uncertainty) from the initial temperature. Equation (1) then determines the propagation velocity v and, along with the values of thermophysical parameters of the sample, the thermal characteristic time is obtained via Eq. (2). The uncertainty in the thermocouple

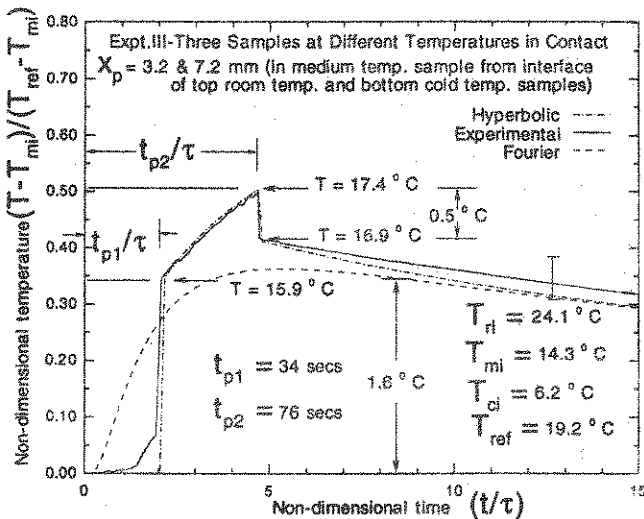


Fig. 4 Experimental results of nondimensional temperature versus time for Experiment III, for thermocouple at $x = 3.2$ and 7.2 mm from interface of room temperature and cold temperature samples, respectively

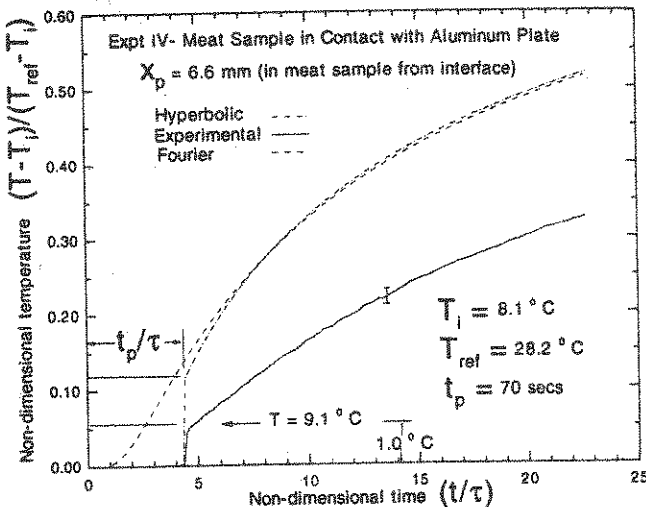


Fig. 5(a) Experimental results of nondimensional temperature versus time for Experiment IV, for thermocouple at $x = 6.6$ mm

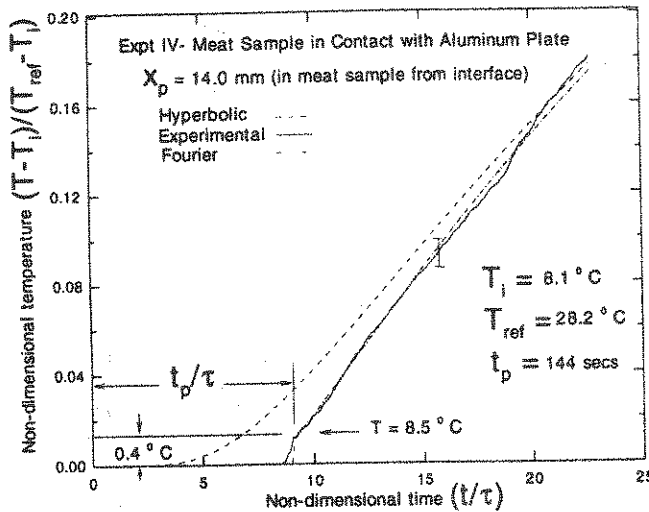


Fig. 5(b) Experimental results of nondimensional temperature versus time for Experiment IV, for thermocouple at $x = 14.0$ mm

dictions. Results similar to Fig. 3(a) for the thermocouple embedded in the middle sample are obtained by Experiment III, the difference being the subtraction of waves due to the superposition of a positive and a negative amplitude wave. These experimental results, presented in Fig. 4, cannot be explained via Fourier theory and are matched only by the hyperbolic non-Fourier model.

Experiment IV, which is different from the previous ones by virtue of the different technique for introducing the jump boundary condition, is examined in Figs. 5(a) and 5(b). The previous experiments relied on the contact between different temperature meat samples to establish the required boundary condition, while Experiment IV uses an aluminum plate that is maintained at a constant temperature via a flow circuit. In Fig. 5(a) for Experiment IV, there is a difference between the experimental data and the theoretical hyperbolic heat conduction curves for the thermocouple at $x = 6.6$ mm. The main problem with this experiment is the inability of the cooling mechanism to instantaneously attain a constant interface temperature between the meat sample and the aluminum plate. During the initial phase of the experiment it is found to be 4–5°C less than the set constant plate temperature. But as time increases, the interface temperature attains that of the specified constant temperature aluminum plate. The experimental data and the theoretical hyperbolic curve match for the thermocouple at $x = 14.0$ mm as shown in Fig. 5(b). This is because

Table 2 Experimentally measured values

Table 2. Experimentally measured values.				
Expt.	TC #	x_p (mm)	t_p (secs)	τ (secs)
I	1	6.3 in room temperature sample	67	15.8
	2	6.6 in cold temperature sample	72	16.6
II	1	3.8 from top cold sample, 1st jump	40	15.3
	2	5.7 from bottom cold sample, 2nd jump	59	15.1
III	1	9.5 from top cold sample at interface	99	15.2
	2	3.2 from room temperature sample, 1st jump	33	14.9
IV	1	7.2 from cold temperature sample, 2nd jump	76	15.6
	2	6.6 from aluminum plate	70	15.8
Mean Value of $\tau = 15.5 \pm 2.1$ seconds (uncertainty = $\pm 13.6\%$).				

the initial deviations of the surface temperature from constant temperature conditions have a lesser influence on the thermocouple further away from the interface due to larger elapsed time as compared to the thermocouple closer to the surface. This is in contrast to Experiments I, II, and III where the theoretical and experimental curves are better matched due to the fact that the interface temperature attains a constant value virtually instantaneously at contact since both cold and warm samples have the same thermal properties. However, the results of the two thermocouples in Experiment IV also show abrupt jumps in temperature and the value of τ obtained from these jumps matches that of the previous experiments. The results of Experiment IV are being presented to show that different techniques yield similar results.

Some possible mechanisms affecting the interpretation of the results within the context of traditional Fourier analysis are examined next. The first is the consideration of thermocouple error. The conservative estimate of uncertainty in the temperature measurement is $\pm 0.2^\circ\text{C}$ (indicated by the error bars of 0.4°C in the corresponding graphs) and that in the time is 0.5 second. Since the measured temperature jumps are consistently much higher than the uncertainty (except for thermocouples placed at large distances from the boundaries where the jump is approximately twice the uncertainty), thermocouple error can be ruled out as a source of the observed trend. In addition, the thermal time constant for the thermocouple is approximately 0.05 second. A second consideration is the effect of thermal contact resistances within a Fourier framework. The jump in temperature that takes place inside the sample may appear to occur due to thermal con-

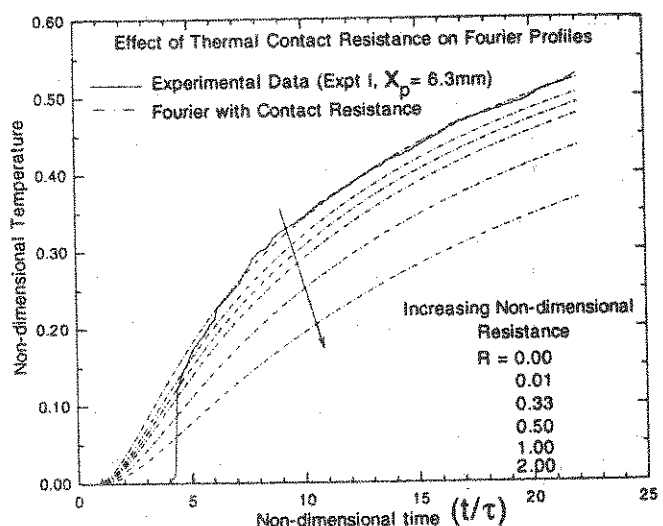


Fig. 6 Effects of thermal contact resistance on Fourier profiles for thermocouple at $x = 6.3$ mm, for Experiment I

τ (secs)
15.8
16.6
15.5
15.1
15.2
14.9
15.6
15.8
15.1

constant
ermocou-
ed time as
This is in
etrical and
t that the
instanta-
have the
two ther-
n temper-
tches that
nt IV are
ld similar

ion of the
is are ex-
ample error.
ture mea-
4°C in the
nd. Since
ch higher
d at large
oximately
d out as a
time con-
nd. A sec-
esistances
that takes
ermal con-

files

dimensional
ce

25

les for ther-

he ASME

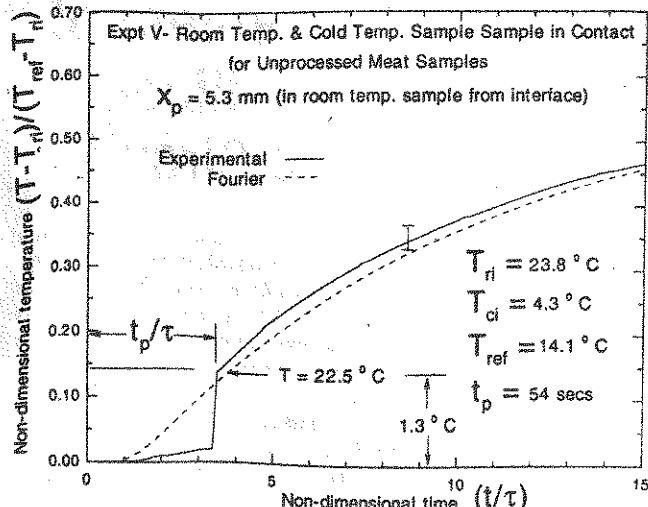


Fig. 7 Results for Experiment V for a thermocouple at $x = 5.3$ mm in room temperature sample for two raw pork meat samples in contact (similar to Experiment I)

tact resistance at the interface. Figure 6 shows the effects of thermal contact resistances on Fourier profiles for one such thermocouple position at $x = 6.3$ mm for Experiment I. The theoretical Fourier profiles for the case of two semi-infinite medium in contact with each other having a thermal contact resistance at the interface are generated using the solution given as (Carslaw and Jaeger, 1959).

$$\theta_1 = \operatorname{erfc} \left[\frac{x}{2\sqrt{\zeta}} \right] - \exp \left(\frac{x}{R} + \frac{\zeta}{R^2} \right) \operatorname{erfc} \left[\frac{x}{2\sqrt{\zeta}} + \frac{\sqrt{\zeta}}{R} \right], \quad (8)$$

where

$$R = \frac{K}{\sqrt{\alpha h_{\text{cont}}}}. \quad (9)$$

Here R is the nondimensional contact resistance and h_{cont} the dimensional contact conductance (inverse of thermal contact resistance). The results for a given thermocouple location of this solution for various nondimensional contact resistances and the experimental results shown in Fig. 6 depict the fact that the jump in temperature that occurs inside the sample cannot be explained by a thermal contact resistance at the interface.

Conclusions

This paper demonstrates experimentally that the *macroscopic* description of the transient heat conduction processes in biological materials is accurately described by a non-Fourier damped wave model rather than a Fourier model. While the actual *microscopic* description of the conduction processes may be represented by more complicated models, the present hyperbolic

non-Fourier description is appropriate for describing *macroscopically* the transient conduction processes in processed meat.

The definitions of the measured thermophysical properties required by the model, such as density, specific heat, and thermal conductivity, remain unchanged from their classical definitions and their magnitudes are obtained by the standard techniques. The values of the thermal characteristic time required by the model are obtained by using these thermophysical properties.

The results and findings presented in the paper have a tremendous impact on the modeling and prediction of bio-heat transfer and lay the foundation for further analyses that will yield better predictive tools for heat and mass transfer processes in complex biological systems. The use of the hyperbolic model of heat conduction, along with the measured values of the thermal characteristic time, for analyzing heat transfer in processed meat (bologna) shows significant difference from traditional Fourier-based results. This indicates that the use of traditional analyses may not be accurate for modeling and predicting heat transfer phenomena in bio-systems. Further research is needed to analyze different kinds of materials, such as the results presented in Fig. 7 for raw pork meat (Experiment V), to establish the effects of hyperbolic conduction in practical applications.

References

- Ascroft, N. W., and Mermin, N. D., 1976, *Solid State Physics*, Saunders Publishing, Philadelphia, PA.
- Carslaw, H. S., and Jaeger, J. C., 1959, *Conduction of Heat in Solids*, Oxford Science Publications, pp. 60–90.
- Cattaneo, C., 1958, "A Form of Heat Conduction Equation Which Eliminates the Paradox of Instantaneous Propagation," *Comptes Rendus*, Vol. 247, pp. 431–433.
- Figliola, R. S., and Beasley, D. E., 1991, *Theory and Design for Mechanical Measurements*, Wiley, pp. 141–178.
- Joseph, D. D., and Preziosi, L., 1989, "Heat Waves," *Reviews of Modern Physics*, Vol. 61, pp. 41–73.
- Joseph, D. D., and Preziosi, L., 1990, "Addendum to the Paper Heat Waves," *Reviews of Modern Physics*, Vol. 62, pp. 375–391.
- Kaminski, W., 1990, "Hyperbolic Heat Conduction Equation for Materials With a Nonhomogeneous Inner Structure," *ASME JOURNAL OF HEAT TRANSFER*, Vol. 112, pp. 555–560.
- Kar, A., Chau, C. L., and Mazumder, J., 1992, "Comparative Studies on Nonlinear Hyperbolic and Parabolic Heat Conduction for Various Boundary Conditions: Analytic and Numerical Solutions," *ASME JOURNAL OF HEAT TRANSFER*, Vol. 114, pp. 14–20.
- Kim, W. S., Hector, L. G., and Özisik, M. N., 1990, "Hyperbolic Heat Conduction Due to Axisymmetric Continuous or Pulse Surface Heat Sources," *Journal of Applied Physics*, Vol. 68, pp. 5478–5485.
- Lavine, A. S., and Bai, C., 1994, "Hyperbolic Heat Conduction in Thin Domains," *Thermal Science and Engineering*, Vol. 2, pp. 185–190.
- Rastegar, S., 1989, "Hyperbolic Heat Conduction in Pulsed Laser Irradiation of Tissue," *Society of Photo-Optical Instrumentation Engineers, Thermal and Optical Interactions With Biological and Related Composite Materials*, Vol. 1064, pp. 114–117.
- Tzou, D. Y., 1992, "Experimental Evidence for the Temperature Waves Around a Rapidly Propagating Crack Tip," *ASME JOURNAL OF HEAT TRANSFER*, Vol. 114, pp. 1042–1045.
- Vedavarz, A., Kumar, S., and Moallemi, M. K., 1994a, "Significance on Non-Fourier Heat Waves in Conduction," *ASME JOURNAL OF HEAT TRANSFER*, Vol. 116, pp. 221–224.
- Vedavarz, A., Mitra, K., and Kumar, S., 1994b, "Hyperbolic Temperature Profiles for Laser Surface Interactions," *Journal of Applied Physics*, to appear.
- Wiggert, D. C., 1977, "Analysis of Early-Time Transient Heat Conduction by Method of Characteristics," *ASME JOURNAL OF HEAT TRANSFER*, Vol. 99, pp. 35–40.
- Zehnder, A. T., and Rosakis, A. J., 1991, "On the Temperature Distribution at the Vicinity of Dynamically Propagating Cracks," *Journal of the Mechanics and Physics of Solids*, Vol. 39, pp. 385–415.